2020 American Control Conference
Denver, CO, USA, July 1-3, 2020

Interval Observer for SOC Estimation in Parallel-Connected Lithium-ion Batteries*

Dong Zhang[1], Luis D. Couto[2], Preet Gill[1], Sebastien Benjamin[3], Wente Zeng[4], and Scott J. Moura[1]

***Abstract*— The internal states of Lithium-ion batteries, notably state of charge (SOC), need to be carefully monitored during battery operation to manage energy and safety. In this paper, we propose an interval observer for SOC estimation in an electrically and thermally coupled parallel connection of cells. This is a particularly challenging problem because mathematically cells in parallel yield a system of differential-algebraic equations (DAE), which are more difficult to handle than ordinary differential equations (e.g. a series string of cells). For a large battery pack with thousands of cells, applying an estimation algorithm on each and every cell would be mathematically and computationally intractable. These issues are tackled using an interval observer based on a coupled equivalent circuit-thermal model. The key novelty lies in considering cell heterogeneity as well as state-dependent parameters as unknown, but with bounded uncertainty. The resulting interval observer maps bounded uncertainties to a feasible set of state estimation, and is independent of the number of cells in parallel. Stability and inclusion of the interval observer are proven and validated through numerical studies.**

I. Introduction

Lithium-ion (Li-ion) batteries play a key role in achieving energy sustainability and reduction in emissions. Li-ion batteries benefit from high energy density, which has motivated their wide use in a variety of applications including electric vehicles and grid energy storage. In recent years, a substantial body of research on real-time control and estimation algorithms for batteries has emerged. However, safe and efficient operation of batteries remains a challenge, especially as the performance requirements of these devices increase.

Large-scale energy storage systems require hundreds to thousands of cells connected in series and parallel to achieve demanded power and voltage [1]. A battery pack's instantaneous power capability is crucial for on-board management and safe operation [2]. However, real-time SOC estimation for a pack is a very intricate task due to (i) limited measurements, (ii) complex electrochemical-thermal-mechanical physics, and (iii) high computational cost [3].

Different battery models for a state observer design have been proposed in the literature, which can be classified into electrochemical white box models [4], [5], equivalent-circuit gray box models [6], [7] and data-driven black box models [8], [9], sorted from high to low physical interpretability. Although each modeling framework has its merits and drawbacks, equivalent circuit models (ECM) provide a reasonable trade-off between complexity and accuracy [6]. ECMs can be made more accurate by increasing the system order to account for additional electrochemical phenomena [10].

An important fact often ignored during battery modeling is the time-varying electrical parameters. In practice, internal parameters, e.g. resistances and capacitance, are non-linearly dependent on the cell's temperature and SOC. High-fidelity temperature models have more accurate predictions, but suffer from high computational cost, rendering them of little use for on-board thermal management [11]. First principles-based two-state thermal model for the cell's core and surface temperatures provide a balanced trade-off between computational efficiency and fidelity [12]. Coupled equivalent circuit-thermal models with temperature dependent parameters have been studied and used for state estimation via an adaptive observer in [13]. Existing techniques for battery pack state estimation includes Luenberger observers [14], Kalman filters [15], unscented Kalman filters [16], and sliding mode observers [17], among others. However, all the previously mentioned techniques require a state observer for each cell, making them computationally intractable for large packs.

In the stochastic estimation/filtering framework, the process and measurement noises are often assumed to be Gaussian. The system characteristics, e.g. mean and variance, are required by filtering algorithms. Nonetheless, the statistical and calibration procedures to obtain these characteristics are often tedious [18]. In contrast, interval estimation [18], [19], [20] assumes that the measurement and process noises are unknown but bounded. In a battery pack with thousands of cells, executing state estimation algorithms based on highly nonlinear and coupled dynamics for every single cell in real time becomes intractable. The interval observer benefits from its scalability by deriving only upper and lower bounds that enclose all unmeasured internal states for all cells in a pack. Previously, only Perez *et al.* designed a sensitivity-based interval observer for single cell SOC estimation from an electrochemical perspective [21], but without provable observer stability and inclusion properties.

Given the aforementioned literature, this paper contributes:

- An analysis of heterogeneous cells connected in parallel, which yields DAEs. Existing studies for cells in series yield ODEs.
- A novel interval observer is designed, given uncertain model parameters, initial conditions, and measurements.

*This work is sponsored by Total S.A. and Saft S.A..

[1]Dong Zhang, Preet Gill, and Scott J. Moura are with Department of Civil and Environmental Engineering, University of California, Berkeley, California, 94720, USA. {dongzhr,preetgill77,smoura}@berkeley.edu

[2]Luis D. Couto is with Department of Control Engineering and System Analysis, Université Libre de Bruxelles, B-1050 Brussels, Belgium. lcoutome@ulb.ac.be

[3]Sebastien Benjamin is with Saft S.A.. Sebastien.BENJAMIN@saftbatteries.com

[4]Wente Zeng is with Total S.A.. wente.zeng@total.com

The remainder of this paper is organized as follows. The coupled electrical-thermal model is developed in Section II, for battery cells connected in parallel. Next, a brief motivation of the problem is presented in Section III. For the reader's convenience, interval observer preliminaries are given in Section IV. The observer design for batteries is pursued in Section V, and followed by an numerical assessment of its performance in Section VI.

Notation. Throughout the manuscript, the symbols Id_n denotes the identity matrix with dimension $n \times n$. For a matrix $A \in \mathbb{R}^{n\times n}$, $\|A\|_{\max} = \max_{i,j=1,2,\cdots,n}|A_{i,j}|$ (the elementwise maximum norm). The relation $Q \succ 0$ ($Q \prec 0$) means that the matrix $Q \in \mathbb{R}^{n\times n}$ is positive (negative) definite. The inner product between $x, y \in \mathbb{R}^n$ is given by $\langle x,y\rangle = \sum_{i=1}^{n} x_i y_i$.

II. Model Development

This section reviews an equivalent-circuit model coupled with a two-state thermal model for a single battery cell, which is then electrically and thermally interconnected with other cell models to form a parallel arrangement of cells.

A. Single Battery Cell

The ECM for a single cell k, consisting of an open circuit voltage (OCV) in series connection with an ohmic resistance and an $R-C$ pair in parallel, is described by

$$\dot{z}_k(t) = \frac{1}{Q_k} I_k(t), \tag{1}$$

$$\dot{V}_{c,k}(t) = -\frac{1}{R_{2,k}(z_k,T_k)C_k(z_k,T_k)} V_{c,k}(t) + \frac{1}{C_k(z_k,T_k)} I_k(t), \tag{2}$$

$$V_k(t) = OCV(z_k(t)) + V_{c,k}(t) + R_{1,k}(z_k,T_k) I_k(t), \tag{3}$$

where $z_k(t)$ represents the SOC for the k-th cell, and $V_{c,k}(t)$ denotes the voltage across the $R_{2,k} - C_k$ pair. Symbol $R_{1,k}$ is the ohmic resistance, and T_k is the cell temperature given by (7). The electrical model parameters, namely $R_{1,k}$, $R_{2,k}$, and C_k, are dependent on SOC and cell temperature, and such dependence can be explicitly characterized via an offline experimental procedure for a cell of interest (see [22] for an example for a $LiFePO_4$/Graphite cell). The output equation (3) for the k-th cell provides the voltage response characterized by a nonlinear open circuit voltage (OCV) as a function of SOC, voltage from the R-C pair, and voltage associated with an ohmic resistance $R_{1,k}$. We specify positive current for charging and negative current for discharging.

A two-state thermal model for a cylindrical cell describes the dynamics of core and surface temperatures [22]:

$$C_c \dot{T}_{c,k}(t) = \dot{Q}_k(t) + \frac{T_{s,k}(t) - T_{c,k}(t)}{R_c}, \tag{4}$$

$$C_s \dot{T}_{s,k}(t) = \frac{T_{f,k}(t) - T_{s,k}(t)}{R_u} - \frac{T_{s,k}(t) - T_{c,k}(t)}{R_c}, \tag{5}$$

$$\dot{Q}_k(t) = \left| I_k(t) \left[V_k(t) - OCV(z_k(t)) \right] \right|, \tag{6}$$

$$T_k(t) = \frac{1}{2}\left(T_{s,k}(t) + T_{c,k}(t)\right), \tag{7}$$

where $T_{c,k}$ and $T_{s,k}$ are the core and surface temperatures for the k-th cell. Symbols R_c, R_u, C_c, and C_s represent heat conduction resistance between core and surface, convection

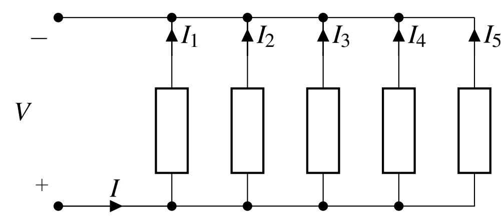

Fig. 1. Parallel connection of five battery cells.

resistance between ambient and surface, core heat capacity, and surface heat capacity, respectively. Symbol $\dot{Q}_k(t) \geq 0$ is the internal heat generation from resistive dissipation. Note that the electrical model (1)-(3) and the thermal model (4)-(7) are coupled via $\dot{Q}_k(t)$ in a nonlinear fashion.

The measured quantities for the coupled electrical-thermal model (1)-(7) are the cell voltage and surface temperature:

$$y_k(t) = \left[V_k(t),\ T_{s,k}(t)\right]. \tag{8}$$

B. Parallel Arrangement of Battery Cells

For a block of m cells in parallel, in order to reduce sensing effort, we assume only the voltage and total current for the block are measured, which is the most realistic scenario. Fig. 1 depicts a parallel connection of $m = 5$ cells. Electrically, Kirchhoff's voltage law constraints terminal voltages to the same value for all cells, which can be mathematically represented by the following nonlinear algebraic constraints

$$OCV(z_i) + V_{c,i} + R_{1,i} I_i = OCV(z_j) + V_{c,j} + R_{1,j} I_j, \quad \forall\ i,j \in \{1,2,\cdots,m\},\ i \neq j. \tag{9}$$

Kirchhoff's current law provides the following linear algebraic constraint,

$$\sum_{k=1}^{m} I_k(t) = I(t), \tag{10}$$

where $I(t)$ is the measured total current, and $I_k(t)$ represents the local current for cell k. It is worth highlighting that (9) imposes $(m-1)$ nonlinear algebraic constraints, whereas (10) imposes one linear algebraic constraint. When only the total current is measured, the local cell currents are unknown. Hence, the system of DAE (1)-(10) must be solved such that the algebraic equations (9) and (10) are fulfilled for all t.

The cells are thermally coupled through coolant flow and heat exchange between adjacent cells [23]. For cell k,

$$C_c \dot{T}_{c,k}(t) = \dot{Q}_k(t) + \frac{T_{s,k}(t) - T_{c,k}(t)}{R_c}, \tag{11}$$

$$C_s \dot{T}_{s,k}(t) = \frac{T_{f,k}(t) - T_{s,k}(t)}{R_u} - \frac{T_{s,k}(t) - T_{c,k}(t)}{R_c} + \frac{T_{s,k-1}(t) + T_{s,k+1}(t) - 2T_{s,k}(t)}{R_{cc}}, \tag{12}$$

$$T_{f,k}(t) = T_{f,k-1}(t) + \frac{T_{s,k-1}(t) - T_{f,k-1}(t)}{R_u C_f}, \tag{13}$$

$$\dot{Q}_k(t) = \left| I_k(t) \left[y_k(t) - OCV(z_k(t)) \right] \right|, \tag{14}$$

$$T_k(t) = \frac{1}{2}(T_{s,k}(t) + T_{c,k}(t)), \tag{15}$$

where $T_{f,k}$ is the coolant flow temperature at the k-th cell, and R_{cc} denotes heat conduction resistance between adjacent battery cell surfaces. Heat conduction between battery cells is driven by the temperature difference between cell surfaces, and this process is described by the third term on the right hand side of (12). Inside the block of m cells in parallel, the coolant flows through individual cells, and the coolant flow temperature at the k-th cell is determined by the flow heat balance of the previous cell, as illustrated in (13). We assume that all the battery cells have the same thermal parameters.

III. Motivation

In this section, we illustrate the heterogeneity for cells in parallel via an open-loop simulation study. Without loss of generality, we consider two $LiNiMnCoO_2$/Graphite (NMC) type cells with 2.8 Ah nominal capacity in parallel. In this embodiment, the cells have identical SOC-OCV relationship, and the heterogeneity arises from:

- Difference in SOC initialization.
- Difference in electrical parameters due to SOC variation.
- Unevenly distributed currents due to parameter variation.
- Difference in temperature due to current variation.

A transient electric vehicle-like charge/discharge cycle generated from the urban dynamometer driving schedule (UDDS) is applied. Specifically, this total applied current (summation of local currents) is plotted in Fig. 2(a).

Two cases are examined here. In the first case, the cells are initialized at the same SOC. Since Cell 2 has higher resistance, its local current is smaller in magnitude relative to local current of Cell 1, as shown in Fig. 2(b) and (c). Figures 2(d) and (e) demonstrate the second case where the cells have different initial SOCs. It can be observed that even though the applied total current is small initially (around zero), Cell 1 takes large negative current (around -10 A) and Cell 2 positions itself at a large positive current (around $+10$ A). This occurs because $z_1(0)$ is initialized higher, and even though the z values for two cells follow a similar trend, they do not synchronize – a bias persists.

In a battery pack composed of hundreds or thousands of heterogeneous cells, executing state estimation algorithms based on a highly nonlinear and coupled model consists of differential-algebraic equations for every single cell in real-time is intractable and not scalable. This motivates our subsequent study on interval observers to increase algorithm scalability and reduce computation and design complexity

IV. Interval Observer Preliminaries

The development of finite-dimensional interval observers based on monotone system theory closely follows the work in [18], [19], [20]. In this section, we review the preliminaries.

Consider the following nonlinear model dynamics [20]:

$$\dot{x} = f(x) + B(\theta(t))u + \delta f(x, \theta(t)), \tag{16}$$

$$y = h(x) + \delta h(\theta(t))u, \tag{17}$$

where $x \in \mathbb{R}^n$ is the state vector, and $u \in \mathbb{R}$ and $y \in \mathbb{R}$ are the system input and output, respectively. The considered system

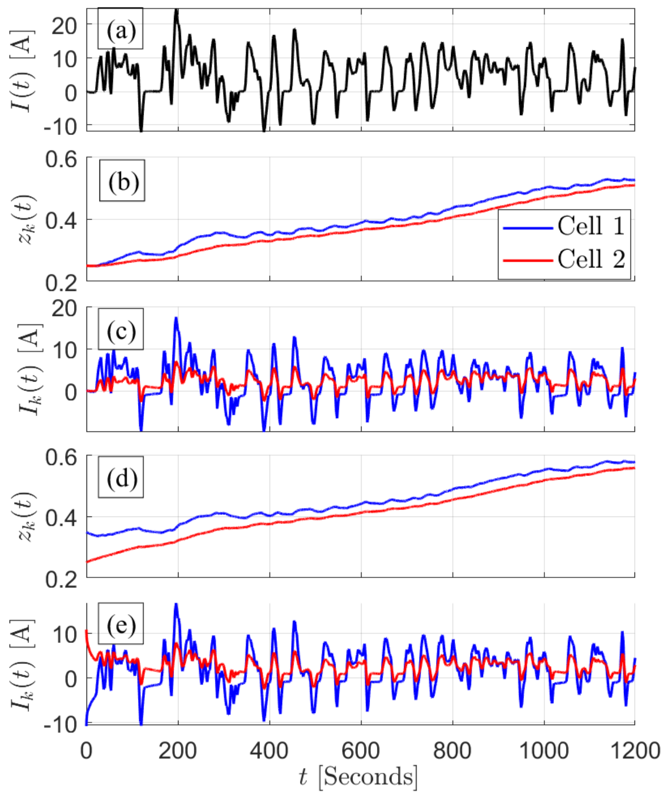

Fig. 2. Simulation results of two cells in parallel using coupled electrical-thermal dynamics with temperature and SOC dependent electrical parameters. In (b)-(c), cells are initialized at the same SOC, and the total current distributes unevenly due to parameter heterogeneity. In (d)-(e), the initial cell SOCs are distinct. The total current again distributes unevenly due to both parameter and initialization heterogeneity.

is single-input-single-output (SISO). The functions $f(x)$ and $h(x)$ are deterministic and smooth, and δf is uncertain and assumed to be locally Lipschitz continuous with respect to x. It is noted that the nominal terms $f(x)$ and $h(x)$ can be freely assigned by the designer via the modification of δf and δh. The initial conditions for the states belong to a compact set $x_0 \in [\underline{x}_0, \overline{x}_0]$, where $\underline{x}_0$ and $\overline{x}_0$ are given. Suppose the uncertain parameters $\theta(t)$ belong to a compact set $\Theta \subset \mathbb{R}^p$, where p is the number of parameters. The values of the parameter vector $\theta(t)$ are not available for measurement, and only the set of admissible values Θ is known. One can obtain a nominal system of (16)-(17) by setting $B = 0$, $\delta f = 0$, and $\delta h = 0$:

$$\dot{x} = f(x), \tag{18}$$

$$y = h(x). \tag{19}$$

According to [18], [24], a time-varying nonlinear and invertible state transformation, based on the Lie derivatives, yields a partial-linear dynamics in the new state coordinate.

Denote the gradient of a scalar field h by $\mathrm{d}h$, and the Lie derivative of h along a vector field f is given by the inner product $L_f h(x) = \langle \mathrm{d}h(x), f(x) \rangle$. High-order Lie derivatives are computed with the iteration $L_f^k h(x) = L_f(L_f^{k-1} h(x))$ where $L_f^0 h(x) = h(x)$. The nominal system (18)-(19) is locally observable around $x = x_e$ if the matrix

$$\mathscr{O}(x_e) = \begin{bmatrix} \mathrm{d}h(x_e) & \mathrm{d}L_f h(x_e) & \cdots & \mathrm{d}L_f^{n-1} h(x_e) \end{bmatrix}^\top \tag{20}$$

has full rank. Under this scenario, the vectors $h(x)$, $L_f h(x)$, $\cdots$, $L_f^{n-1}h(x)$ form the new coordinate for the states in a neighborhood of x defined by

$$\Phi(x) = \begin{bmatrix} \phi_1(x) \\ \phi_2(x) \\ \vdots \\ \phi_n(x) \end{bmatrix} = \begin{bmatrix} h(x) \\ L_f h(x) \\ \vdots \\ L_f^{n-1}h(x) \end{bmatrix}, \tag{21}$$

and the transformation map $\xi = \Phi x$ is a local diffeomorphism. The coordinate transformation obtained from the locally observable nominal system (18)-(19) is then utilized to transform the original uncertain system (16)-(17) into a partial-linear expression

$$\dot{\xi} = A_0\xi + \delta A(\theta)\xi + b(\xi,\theta), \tag{22}$$
$$y = H\xi + v(\theta,t), \tag{23}$$

where $v(\theta,t) = \delta h(\theta)u$. The matrix $A_0 \in \mathbb{R}^n$ is deterministic and the matrix $\delta A(\theta) \in \mathbb{R}^n$ represents the uncertain part inherited from the uncertain nonlinear system (16)-(17). Symbol $b(\xi,\theta)$ indicates a lumped uncertain nonlinear function. Since $\theta \in \Theta$, the following assumptions will be used.

Assumption 1: $\underline{\delta A} \le \delta A(\theta) \le \overline{\delta A}$, $\underline{b}(t) \le b(\xi,\theta) \le \overline{b}(t)$, $\left|v(\theta,t)\right| \le V(t)$, for all $\theta \in \Theta$ and $t \ge 0$.
We then introduce the following definition.

Definition 1 ([19]): For a matrix $\mathscr{A} \in \mathbb{R}^{n\times n}$, define $\mathscr{A}^+ = \max\{0,\mathscr{A}\}$ and $\mathscr{A}^- = \mathscr{A}^+ - \mathscr{A}$. For a vector $\xi \in \mathbb{R}^n$, define $\xi^+ = \max\{0,\xi\}$ and $\xi^- = \xi^+ - \xi$.

According to Assumption 1 and Definition 1, the following lemma is then realized.

Lemma 1 ([19]): Let $\underline{\delta A} \le \delta A(\theta) \le \overline{\delta A}$ for some $\underline{\delta A}, \delta A, \overline{\delta A} \in \mathbb{R}^{n\times n}$, and $\underline{\xi} \le \xi \le \overline{\xi}$ for $\underline{\xi}, \overline{\xi}, \xi \in \mathbb{R}^n$, then

$$\begin{aligned}\delta A(\theta)\cdot\xi \in &[\underline{\delta A}^+\underline{\xi}^+ - \overline{\delta A}^+\underline{\xi}^- - \underline{\delta A}^-\overline{\xi}^+ + \overline{\delta A}^-\overline{\xi}^-, \\ &\overline{\delta A}^+\overline{\xi}^+ - \underline{\delta A}^+\overline{\xi}^- - \overline{\delta A}^-\underline{\xi}^+ + \underline{\delta A}^-\underline{\xi}^-].\end{aligned} \tag{24}$$

For a vector $L \in \mathbb{R}^n$, system (22)-(23) can be rewritten as

$$\dot{\xi} = (A_0 - LH)\xi + \delta A(\theta)\xi + b(\xi,\theta) + L(y - v), \tag{25}$$

The following interval observer structure is proposed [19],

$$\begin{aligned}\dot{\underline{\xi}} =&(A_0 - LH)\underline{\xi} + (\underline{\delta A}^+\underline{\xi}^+ - \overline{\delta A}^+\underline{\xi}^- - \underline{\delta A}^-\overline{\xi}^+ + \overline{\delta A}^-\overline{\xi}^-) \\ &+ \underline{L}y - |\underline{L}|V(t) + \underline{b}(t),\end{aligned} \tag{26}$$

$$\begin{aligned}\dot{\overline{\xi}} =&(A_0 - LH)\overline{\xi} + (\overline{\delta A}^+\overline{\xi}^+ - \underline{\delta A}^+\overline{\xi}^- - \overline{\delta A}^-\underline{\xi}^+ + \underline{\delta A}^-\underline{\xi}^-) \\ &+ \overline{L}y + \left|\overline{L}\right|V(t) + \overline{b}(t)\end{aligned} \tag{27}$$

The following theorem provides a sufficient condition for stability and enclosure of the interval observer design.

Theorem 1 ([19]): Let Assumption 1 be satisfied and the matrices $(A_0 - \underline{L}H)$ and $(A_0 - \overline{L}H)$ are Metzler. Then $\underline{\xi}(t) \le \xi(t) \le \overline{\xi}(t)$, $\forall\, t \ge 0$ is satisfied provided that $\underline{\xi}_0 \le \xi_0 \le \overline{\xi}_0$. Furthermore, if there exists $P \in \mathbb{R}^{2n\times 2n}$, $P = P^\top \succ 0$ and $\gamma > 0$ such that the following Riccati matrix inequality is verified

$$G^\top P + PG + 2\gamma^{-2}P^2 + \gamma^2\eta^2 Id_{2n} + Z^\top Z \prec 0, \tag{28}$$

where $\eta = 2n\|\overline{\delta A} - \underline{\delta A}\|_{\max}$, $Z \in \mathbb{R}^{s\times 2n}$, $0 < s \le 2n$ and

$$G = \begin{bmatrix} A_0 - \underline{L}H + \underline{\delta A}^+ & -\underline{\delta A}^- \\ -\overline{\delta A}^- & A_0 - \overline{L}H + \overline{\delta A}^+ \end{bmatrix}, \tag{29}$$

then $\underline{\xi}$, $\overline{\xi} \in \mathscr{L}_\infty^n$. Moreover,

$$\underline{x} = \inf\left(\Phi^{-1}(\eta)\right), \quad \overline{x} = \sup\left(\Phi^{-1}(\eta)\right), \tag{30}$$

where $\eta \in \left[\underline{\xi}, \overline{\xi}\right]$.

The proof for Theorem 1 is omitted here. Interested readers may refer to [19] Theorem 7 for more details. We translate this theory to battery pack state estimation next.

V. Interval Observer for Batteries

In this section, the interval observer design introduced in Section IV is applied to the Li-ion battery state estimation problem. We examine two scenarios – (i) a single battery cell with temperature and SOC-dependent electrical parameters; (ii) electrically and thermally coupled cells in parallel, with SOC and temperature-dependent electrical parameters.

A. Single Battery Cell

It is hereby assumed that the input current, terminal voltage and surface temperature of the k-th single cell are experimentally measured. Ideally, a deterministic state observer could be proposed for the state estimation of the coupled nonlinear electrical-thermal system (1)-(8). However, this approach is intractable due to the system nonlinearities like electrical-thermal coupling, state-dependent parameters and voltage output function. To tackle this issue, we suppress the electrical parameters' dependence on the internal states, and treat these parameters as uncertain. Specifically, $\theta \in \Theta \subset \mathbb{R}^4$, where $\theta = \begin{bmatrix} R_{1,k} & R_{2,k} & C_k & Q_k \end{bmatrix}^\top$. The objective is to design a robust interval observer, using the measurements, to determine the set of admissible values for cell SOC at each time instant, when the plant model is subject to bounded uncertainties in the parameters and states' initial conditions.

Let $\tau_k = 1/(R_{2,k}C_k)$, and consider a known nominal value $\tau_{k,0}$ such that $\tau_k = \tau_{k,0} + \delta\tau_k$, where $\tau_{k,0}$ is a deterministic scalar and $\delta\tau_k$ represents the uncertain component. The single cell electrical system (1)-(3) can thus be formulated in terms of uncertain system (16)-(17), with

$$\begin{aligned} &x = \begin{bmatrix} x_1 \\ x_2 \end{bmatrix} = \begin{bmatrix} z_k \\ V_{c,k} \end{bmatrix},\ f(x) = \begin{bmatrix} 0 \\ -\tau_{k,0}x_2 \end{bmatrix}, \\ &\delta f(x,\theta) = \begin{bmatrix} 0 \\ -\delta\tau_k x_2 \end{bmatrix},\ B(\theta) = \begin{bmatrix} \frac{1}{Q_k} \\ \frac{1}{C_k} \end{bmatrix},\ u = I_k(t), \\ &h(x) = OCV(x_1) + x_2,\ \delta h(\theta) = R_{1,k}. \end{aligned} \tag{31}$$

It is assumed that the following upper and lower bounds are imposed on the uncertain parameters, i.e. $Q_k \in \left[\underline{Q}, \overline{Q}\right]$, $C_k \in \left[\underline{C}, \overline{C}\right]$, $\delta\tau_k \in \left[\underline{\delta\tau}, \overline{\delta\tau}\right]$, $R_{1,k} \in \left[\underline{R}_{1,k}, \overline{R}_{1,k}\right]$, so that Θ is a four-dimensional polytope. These bounds might be found in practice through parameter identification of the weakest and strongest cells in the pack. The local observability matrix for the nominal system is then given by

$$\mathscr{O}(x)=\begin{bmatrix}\mathrm{d}h(x)\\ \mathrm{d}L_f h(x)\end{bmatrix}=\begin{bmatrix}\frac{\mathrm{d}OCV}{\mathrm{d}x_1}(x_1) & 1\\ 0 & -\tau_{k,0}\end{bmatrix}, \quad (32)$$

whose rank is 2 if and only if the first derivative of the OCV function with respect to SOC is non-zero around an equilibrium point $x_1 = x_{1,e}$ and $\tau_{k,0} \neq 0$, i.e.

$$\frac{\mathrm{d}OCV}{\mathrm{d}x_1}(x_{1,e}) \neq 0, \quad \tau_{k,0} \neq 0 \quad (33)$$

which aligns with existing results on local observability for battery models [3]. Hence, the coordinate transformation based on Lie algebra

$$\Phi(x)=\begin{bmatrix}\xi_1\\ \xi_2\end{bmatrix}=\begin{bmatrix}OCV(x_1)+x_2\\ -\tau_{k,0}x_2\end{bmatrix} \quad (34)$$

transforms the system (16), (17), with (31) to the nonlinear parameter-varying system (22)-(23), with

$$A_0=\begin{bmatrix}0 & 1\\ 0 & -\tau_{k,0}\end{bmatrix},\quad \delta A(\theta)=\begin{bmatrix}0 & \frac{\delta\tau_k}{\tau_{k,0}}\\ 0 & -\delta\tau_k\end{bmatrix},\quad H=\begin{bmatrix}1 & 0\end{bmatrix},$$

$$b(\xi,\theta)=\begin{bmatrix}\frac{1}{Q_k}\varphi\left(\xi_1+\frac{1}{\tau_{k,0}}\xi_2\right)+\frac{1}{C_k}\\ -\frac{\tau_{k,0}}{C_k}\end{bmatrix}I, \quad (35)$$

where

$$\varphi(\cdot)=\frac{\mathrm{d}OCV}{\mathrm{d}x}(OCV^{-1}(\cdot)). \quad (36)$$

An interval observer can be designed based on (26)-(27) and Theorem 1. The bounding functions $\overline{\delta A}$ and $\underline{\delta A}$ for δA can be readily obtained by applying the parameter bounds. The bounding functions $\overline{b}(t)$ and $\underline{b}(t)$ are carefully evaluated according to the direction of current $I(t)$ for all t.

B. Battery Cells in Parallel

As opposed to having one interval observer for a single cell in the preceding discussion, the proposed design is generalized for a cluster of battery cells in parallel. One practical advantage for using an interval observer for a group of cells is scalabilty. An interval observer, composed of only two dynamical systems estimating upper and lower bounds that all trajectories of unknown states live in, significantly reduces computation and design effort. Due to cell heterogeneity, an interval observer constructs two trajectories that upper and lower bound all SOC trajectories, without dealing with the differential-algebraic nature of the circuit dynamics.

The interval observer design for parallel cells inherits the essence of the design for single cells. The only difference is to compute a single set of bounding functions that bound uncertainties from each cell in the parallel configuration.

Remark 1: A crucial step in designing interval observers for cells in parallel is to find the bounding functions for the uncertainties. Namely, the bounding functions are closely associated with the instantaneous bounds on the local currents. Unlike the single cell scenario, the local currents of parallel cells are not available for measurement. In this work, we assume that appropriate bounds on the local currents are given. This issue will be addressed in future work.

Remark 2: The width/tightness of the estimated intervals is dependent on the magnitude of model uncertainties, and our knowledge of the uncertainties when defining the bounding functions.

VI. Simulation Studies

In order to validate the interval observer design, numerical studies are carried out on NMC battery cells modeled with a lumped electrical-thermal model (1)-(10). The state-dependent electrical model parameters are taken from [22]. The total current fed to the battery is a UDDS driving cycle. The interval observer from Theorem 1 is used to estimate the bounds on the internal states from only total current and voltage measurements. Two scenarios are considered. First, the state estimation of a single battery cell is tested, which accounts for uncertainties linked to state dependent parameters. Then, the same observer is used to estimate the state interval for a parallel arrangement of five cells, which involves uncertainty due to cell heterogeneity as well as SOC and temperature dependent parameters.

A. Interval Observer for Single Battery Cell

Let us first consider a single cell and design the interval observer according to Section V-A. The initial value for SOC in the plant model is 30%, and the initial values on the interval observers (lower and upper bounds) are 20% and 40%. The observer gains are chosen to be $\underline{L}=[10 \;\; -0.1]^\top$ and $\overline{L}=[10 \;\; -0.1]^\top$, which ensure that $(A_0-\underline{L}H)$ and $(A_0-\overline{L}H)$ are Metzler and Hurwitz. The black signal in Fig. 3(a) shows the applied current. The solid black curve in Fig. 3(b) is the plant model simulated SOC, and the shaded green region represents feasible SOC values between the estimated intervals. From these plots, the interval observer recovers quickly (less than 20 s) from large initial errors and always enclose the true SOC of the battery. These results confirm the stability and inclusion properties of the designed interval observer stated in Theorem 1, given uncertain initial conditions and state-dependent parameters.

B. Interval Observer for Battery Cells in Parallel

Let us now consider a parallel arrangement of five cells, which differ in their initial SOCs and model parameters. The interval observer is designed according to V-B. The initial SOCs are 20%, 30%, 34%, 37%, and 49%, and the initial bounds (interval observer) on SOCs are 15% and 54%. The applied total current is given by the orange signal in Fig. 3(a). In Fig. 3(c), the solid curves represent the true SOC of each cell, and the shaded green area highlights the feasible SOC values for all cells between the estimated intervals. These plots show that the interval observer is close to the minimum and maximum states during its temporal evolution. It also envelops the state distribution across the five cells. Hence, the results show that cell heterogeneity can be included as unknown but bounded uncertainties, which is exploited to develop an interval observer that provides reliable bound

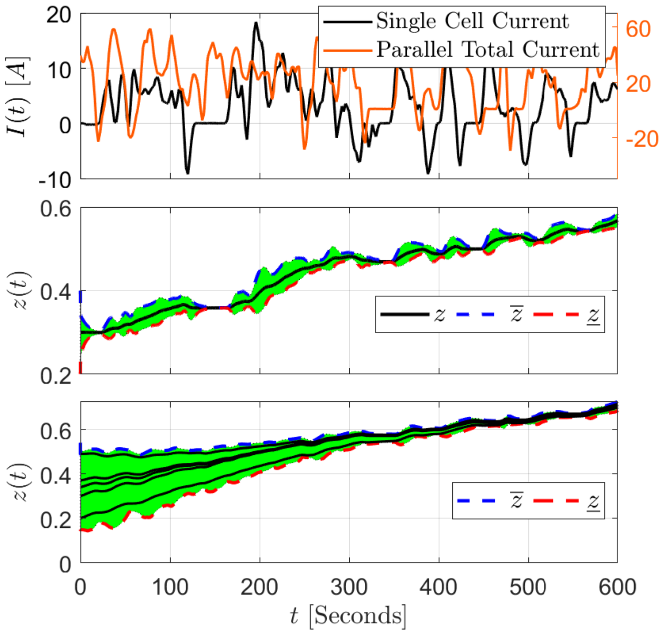

Fig. 3. The interval observer bounds enclose the true states of charge for (b) a single cell and (c) five cells in parallel.

estimates for the states. Moreover, stability and inclusion of the observer are guaranteed by Theorem 1.

VII. Conclusions

An interval observer based on an equivalent circuit-thermal model for lithium-ion batteries has been presented in this paper. The SOC-temperature-dependent parameters are considered as unknown but bounded uncertainties. Then, a parallel arrangement of five cells is used for observer design, where cell heterogeneity is now accounted for through the uncertainty bounding functions. Given that the nominal battery model is locally observable, the original uncertain model can be transformed into a partial-linear form, which enables interval estimation based on monotone systems. By properly choosing the observer gains, the state matrix of the estimation error is Hurwitz and Metzler, which guarantees stability and inclusion of the state bound estimates. A major feature of the proposed estimation approach is its scalability, since the number of states of interval observers is independent of the number of cells. Simulation showcases the effectiveness of the interval observer design. Future work includes developing a systematic methodology for computing the bounding functions associated with unknown local currents.

VIII. Acknowledgement

Luis D. Couto would like to thank the Wiener-Anspach Foundation for its financial support.

References

[1] Michael A Roscher, Oliver S Bohlen, and Dirk Uwe Sauer. Reliable state estimation of multicell lithium-ion battery systems. *IEEE Transactions on Energy Conversion*, 26(3):737–743, 2011.

[2] Kandler Smith and Chao-Yang Wang. Power and thermal characterization of a lithium-ion battery pack for hybrid-electric vehicles. *Journal of power sources*, 160(1):662–673, 2006.

[3] Shi Zhao, Stephen R Duncan, and David A Howey. Observability analysis and state estimation of lithium-ion batteries in the presence of sensor biases. *IEEE Transactions on Control Systems Technology*, 25(1):326–333, 2016.

[4] Nalin A Chaturvedi, Reinhardt Klein, Jake Christensen, Jasim Ahmed, and Aleksandar Kojic. Algorithms for advanced battery-management systems. *IEEE Control systems magazine*, 30(3):49–68, 2010.

[5] Dong Zhang, Satadru Dey, Luis D Couto, and Scott J Moura. Battery adaptive observer for a single-particle model with intercalation-induced stress. *IEEE transactions on control systems technology*, 2019.

[6] Xiaosong Hu, Shengbo Li, and Huei Peng. A comparative study of equivalent circuit models for Li-ion batteries. *Journal of Power Sources*, 198:359–367, 2012.

[7] Dong Zhang, Satadru Dey, Hector E Perez, and Scott J Moura. Remaining useful life estimation of lithium-ion batteries based on thermal dynamics. In *American Control Conference (ACC)*, pages 4042–4047, 2017.

[8] Saehong Park, Dong Zhang, and Scott Moura. Hybrid electrochemical modeling with recurrent neural networks for Li-ion batteries. In *American Control Conference (ACC)*, pages 3777–3782, 2017.

[9] Freeman Rufus, Seungkoo Lee, and Ash Thakker. Health monitoring algorithms for space application batteries. In *International Conference on Prognostics and Health Management*, pages 1–8, 2008.

[10] Saeed Sepasi, Reza Ghorbani, and Bor Yann Liaw. A novel on-board state-of-charge estimation method for aged Li-ion batteries based on model adaptive extended Kalman filter. *Journal of Power Sources*, 245:337–344, 01 2014.

[11] Tarun Huria, Massimo Ceraolo, Javier Gazzarri, and Robyn Jackey. High fidelity electrical model with thermal dependence for characterization and simulation of high power lithium battery cells. *IEEE International Electric Vehicle Conference (IEVC)*, 2012.

[12] Xinfan Lin, Hector E Perez, Jason B Siegel, Anna G Stefanopoulou, Yonghua Li, R Dyche Anderson, Yi Ding, and Matthew P Castanier. Online parameterization of lumped thermal dynamics in cylindrical lithium ion batteries for core temperature estimation and health monitoring. *IEEE Transactions on Control Systems Technology*, 21(5):1745–1755, 2012.

[13] Xinfan Lin, Hector Perez, Jason Siegel, Anna Stefanopoulou, Yi Ding, and Matthew Castanier. Parameterization and observability analysis of scalable battery clusters for onboard thermal management. *Oil & Gas Science and Technology*, 68(1):165–178, 2013.

[14] Xiaosong Hu, Fengchun Sun, and Yuan Zou. Estimation of state of charge of a lithium-ion battery pack for electric vehicles using an adaptive Luenberger observer. *Energies*, 3(9):1586–1603, 2010.

[15] Gregory Plett. Extended Kalman filtering for battery management systems of LiPB-based HEV battery packs: Part 1. Background. *Journal of Power Sources*, 134:252–261, 2004.

[16] Luis D Couto and Michel Kinnaert. Partition-based unscented Kalman filter for reconfigurable battery pack state estimation using an electrochemical model. In *American Control Conference (ACC)*, pages 3122–3128, 2018.

[17] Taesic Kim, Wei Qiao, and Liayn Qu. Online SOC and SOH estimation for multicell lithium-ion batteries based on an adaptive hybrid battery model and sliding-mode observer. In *IEEE Energy Conversion Congress and Exposition*, pages 292–298, 2013.

[18] Tarek Raïssi, Denis Efimov, and Ali Zolghadri. Interval state estimation for a class of nonlinear systems. *IEEE Transactions on Automatic Control*, 57(1):260–265, 2011.

[19] Stanislav Chebotarev, Denis Efimov, Tarek Raïssi, and Ali Zolghadri. Interval observers for continuous-time LPV systems with L1/L2 performance. *Automatica*, 58:82–89, 2015.

[20] Gang Zheng, Denis Efimov, and Wilfrid Perruquetti. Design of interval observer for a class of uncertain unobservable nonlinear systems. *Automatica*, 63:167–174, 2016.

[21] Hector E Perez and Scott J Moura. Sensitivity-based interval PDE observer for battery SOC estimation. In *American Control Conference (ACC)*, pages 323–328, 2015.

[22] Xinfan Lin, Hector E Perez, Shankar Mohan, Jason B Siegel, Anna G Stefanopoulou, Yi Ding, and Matthew P Castanier. A lumped-parameter electro-thermal model for cylindrical batteries. *Journal of Power Sources*, 257:1–11, 2014.

[23] Xinfan Lin, Yi Ding, Matthew P Castanier, and Anna G Stefanopoulou. Estimating core temperatures of battery cells in a battery pack, May 28 2015. US Patent App. 14/403,057.

[24] Alberto Isidori. *Nonlinear control systems*. Springer Science & Business Media, 2013.